

Thin-film CuInSe₂/CdS heterojunction solar cells

L. L. Kazmerski, F. R. White, and G. K. Morgan

Citation: *Appl. Phys. Lett.* **29**, 268 (1976); doi: 10.1063/1.89041

View online: <http://dx.doi.org/10.1063/1.89041>

View Table of Contents: <http://apl.aip.org/resource/1/APPLAB/v29/i4>

Published by the American Institute of Physics.

Related Articles

Efficiency enhancement of organic photovoltaic devices using a Sm:Al compound electrode
Appl. Phys. Lett. **102**, 073301 (2013)

Efficiency enhancement of organic photovoltaic devices using a Sm:Al compound electrode
APL: Org. Electron. Photonics **6**, 33 (2013)

Correlation between interface energetics and open circuit voltage in organic photovoltaic cells
Appl. Phys. Lett. **101**, 233301 (2012)

Correlation between interface energetics and open circuit voltage in organic photovoltaic cells
APL: Org. Electron. Photonics **5**, 259 (2012)

New method to assess the loss parameters of the photovoltaic modules
J. Renewable Sustainable Energy **4**, 063115 (2012)

Additional information on *Appl. Phys. Lett.*

Journal Homepage: <http://apl.aip.org/>

Journal Information: http://apl.aip.org/about/about_the_journal

Top downloads: http://apl.aip.org/features/most_downloaded

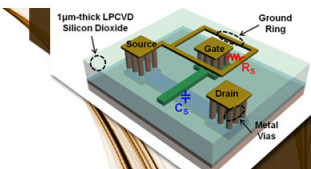
Information for Authors: <http://apl.aip.org/authors>

ADVERTISEMENT

AIP | Applied Physics
Letters


**EXPLORE WHAT'S
NEW IN APL**

SUBMIT YOUR PAPER NOW!



**SURFACES AND
INTERFACES**

Focusing on physical, chemical, biological, structural, optical, magnetic and electrical properties of surfaces and interfaces, and more...



**ENERGY CONVERSION
AND STORAGE**

Focusing on all aspects of static and dynamic energy conversion, energy storage, photovoltaics, solar fuels, batteries, capacitors, thermoelectrics, and more...

Thin-film $\text{CuInSe}_2/\text{CdS}$ heterojunction solar cells*

L. L. Kazmerski, F. R. White,[†] and G. K. Morgan

Department of Electrical Engineering, University of Maine, Orono, Maine 04473
(Received 8 April 1976)

The fabrication procedures and characteristics of several thin-film $p\text{-CuInSe}_2/n\text{-CdS}$ heterojunction solar cells are presented. Two modes of operation (illumination through CuInSe_2 or through CdS) are discussed. Efficiencies in the range of 4–5% are reported, under 100 mW/cm^2 tungsten-halogen illumination for 1.2-cm^2 devices. Included are the spectral response and J - V characteristics for these photovoltaic junctions.

PACS numbers: 84.60.Jt, 85.60.Me, 72.40.+w

Several I-III-VI₂ ternary semiconductors have been receiving increased attention lately, primarily due to their photovoltaic device potential.^{1–4} Among these chalcopyrite-type materials, CuInSe_2 possesses some exceptional characteristics for heterojunction application with CdS . These factors include: (i) CuInSe_2 is a direct band-gap semiconductor which minimizes the requirements for minority-carrier diffusion lengths.⁵ (ii) The lattice match between CuInSe_2 and hexagonal CdS is exceptionally good.⁴ (The difference in the relevant lattice parameters of 0.07 \AA , or a mismatch of approximately 1.2%, introduces only a small amount of interfacial defects.) (iii) Thin films of CuInSe_2 can be produced, either n or p type, by vacuum deposition.⁶ (iv) The energy gap, 1.04 eV, of CuInSe_2 is near an optimal value for terrestrial conditions.⁷ And finally, (v) the electron affinities of CuInSe_2 and CdS are close enough to minimize any potential barriers to the photo-induced carriers.⁴

An important demonstration of the feasibility of this heterojunction has been reported recently by Shay *et al.*⁴ Their device, consisting of a $p\text{-CuInSe}_2$ single crystal and an evaporated CdS film, had a measured efficiency in excess of 12%. This is especially significant since only three other material systems (Si , GaAs / $\text{Ga}_x\text{Al}_{1-x}\text{As}$, and InP/CdS) have demonstrated efficiencies greater than 10%. In the present letter, the first report of a thin film $\text{CuInSe}_2/\text{CdS}$ heterojunction solar cell, with efficiencies in the 4–5% range, is presented.

Two fabrication techniques and two modes of device operation have been successfully utilized. *Mode I*: illumination through the CuInSe_2 . For this operational mode, two methods of junction formation have been developed: (i) Etched Junction, in which the CdS layer is deposited directly onto a metallized substrate. This layer, approximately $6\text{--}8 \mu$ in thickness, is then etched in a dilute (10% HCl) solution subsequent to removal from the vacuum system. A thin ($0.25\text{--}0.50 \mu$) CuInSe_2 is then grown on the CdS using a two-source ($\text{CuInSe}_2 + \text{Se}$) technique⁸ in order to control carrier type. (ii) *In Situ* fabrication, in which the complete process is accomplished without breaking the vacuum. It should be noted that if the initial CdS film is cooled and exposed to the environment, no photovoltaic effect results unless the CdS layer is etched just prior to CuInSe_2 deposition. *Mode II*: Illumination through the CdS . Since the CdS has a band gap of 2.42 eV (300 K), it acts as a window for the solar radiation. Thus, a $p\text{-CuInSe}_2$ film is grown on a Au-metallized glass substrate, by the two-source

technique. The CdS film (in this case about 6μ) is grown directly on the CuInSe_2 ($5\text{--}6 \mu$) without breaking the vacuum.

In all cases, the substrate temperatures were held at 500 K for CdS deposition and 525 K for the CuInSe_2 . The CdS resistivity was of the order of $10 \Omega\text{cm}$. Grain sizes were in the range $0.8\text{--}1.2 \mu$ for both film types. A "fingered" contact configuration was used as the top electrode (Al on CdS and Au-Ag paste on CuInSe_2). The devices were of the order of 1 cm^2 in area. Each device was subjected to a short bake (15–20 min) at 450 K in a 10^{-1} Pa vacuum before measurements were taken.

Figure 1 shows the light and dark characteristics for two devices operating in mode I. Typically, the *in situ* produced junctions [Fig. 1(b)] had higher efficiencies and fill factors than the etched junctions [Fig. 1(a)]. This is attributed to the higher series resistance probably resulting from surface states present from the atmosphere exposure—etching process. The illumination was a tungsten-halogen source set at an intensity at 100 mW/cm^2 as calibrated by a $\text{Cu}_2\text{S/CdS}$ solar cell standard (ERDA/NASA Z66). In each case, the short-

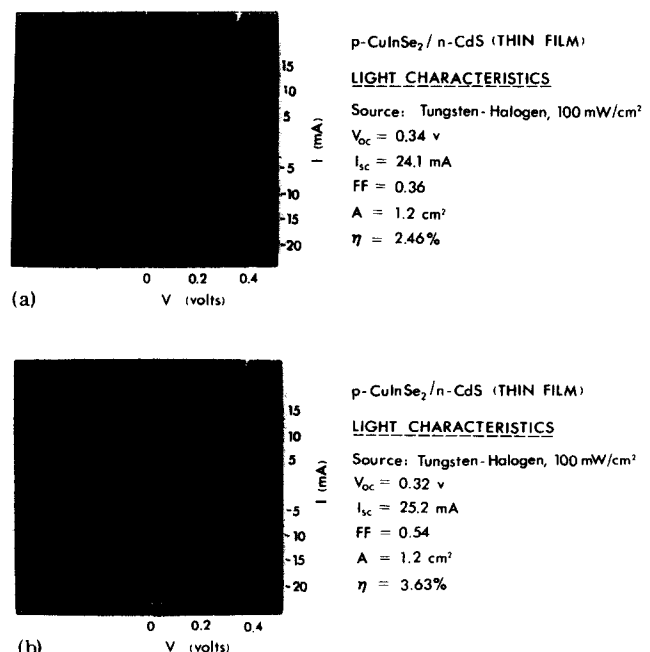


FIG. 1. Light and dark I - V characteristics for $\text{CuInSe}_2/\text{CdS}$ heterojunction, mode I operation. (a) Etched junction; (b) *in situ* produced junction. Measurements made at 300 K.

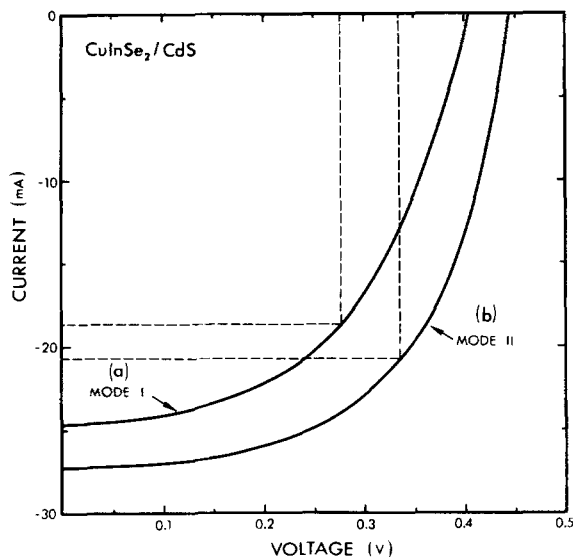


FIG. 2. Comparison of devices in (a) mode I and (b) mode II operations. Illumination is tungsten-halogen at 100 mW/cm². Device temperature, 300°K; Device areas 1.2 cm².

circuit currents are very good, but the open-circuit voltages are somewhat disappointing (~0.35 V compared to 0.55 V reported by Shay.⁴)

Figure 2 presents a comparison of the "best" to-date mode I device (*in situ* produced, $\eta = 4.4\%$) with a mode II device ($\eta = 5.7\%$). Although a higher V_{oc} (=0.44 V) is obtained in the latter case, it is still below that obtained by Shay. The greater efficiency on mode II operation can be attributed to the better absorption of carriers via the CdS window and an improved junction characteristic. A spectral response characteristic for a typical mode II device is shown in Fig. 3. (The mode I response is similar.) The quantum efficiency is fairly flat (~55%) over the range $0.58 < \lambda < 1.3 \mu$. The two observable cutoffs are attributed to (i) low wavelength absorption by the CdS; (ii) high wavelength absorption limit of the CuInSe₂.

Finally, forward J - V characteristics are shown in Fig. 4 for (a) the etched junction, and (b) *in situ* junction.

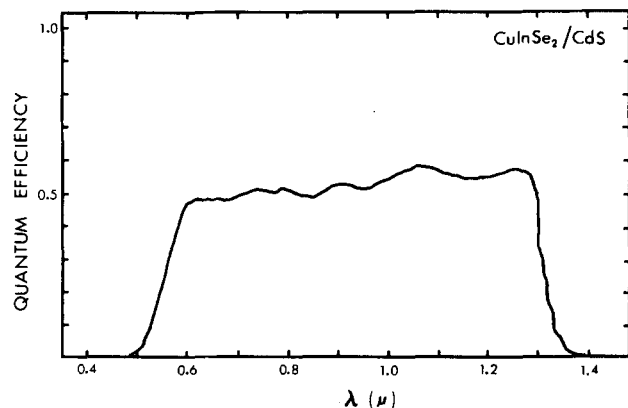


FIG. 3. Spectral response characteristics for CuInSe₂/CdS heterojunction.

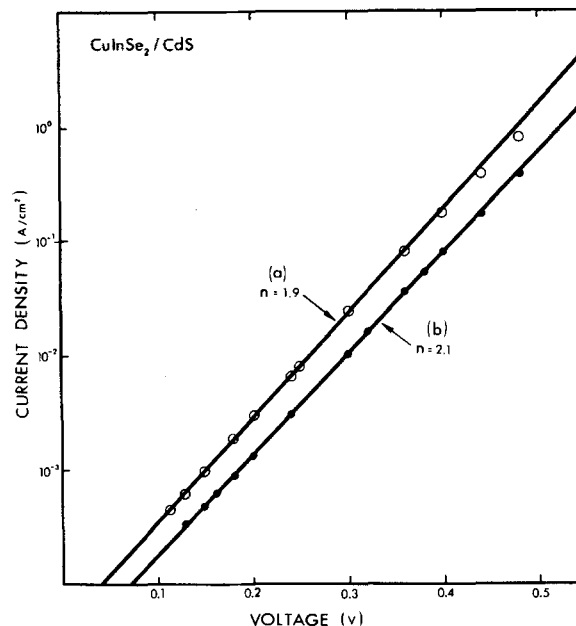


FIG. 4. Dependence of current density on voltage (forward characteristic) indicating $J \propto \exp(qV/nkT)$ for CuInSe₂/CdS diodes. (a) Etched junction; (b) *in situ* junction.

tion. J varies as $\exp(qV/nkT)$ in each case, where $\eta = 1.9$ for the etched junction and $n = 2.1$ for the *in situ* junction. Therefore, the generation-recombination process dominates, as expected, for these thin-film diodes.^{10,11}

The stability of this solar cell has not been investigated in detail. No degradation has been noticed over a rather short time period (weeks). It is suggested, however, that the stability might be better than that of its Cu₂S/CdS counterpart. The reasons for this suggestion rely on the comparison of the crystal structures of CuInSe₂ and Cu₂S. The chalcopyrite structure is relatively simple compared to the Cu₂S chalcocite phase. Since the degradation of the Cu₂S/CdS cell is attributed to Cu migration and Cu₂S-phase deterioration,⁹ the use of CuInSe₂ might lead to greater reliability since only a single phase of CuInSe₂ exists at low temperatures, and the Cu atoms are more tightly bound in the Cu-In-Se chalcopyrite lattice.

In conclusion, the fabrication of a thin-film p -CuInSe₂/ n -CdS heterojunction solar cell, with efficiencies of the order 4–5% has been demonstrated. The future development of these devices depends on the improvement of the open-circuit voltages to at least the reported 0.55-V magnitude. The adjustment of film grain sizes and/or the use of a mixed CdS/ZnS layer might be investigated in order to improve this parameter. Since the development of this device is still in its initial states, the CuInSe₂/CdS solar cell might prove to be a viable alternative to present thin-film devices in light of this reported progress. This premise is reinforced by the fact that the reported efficiency of this 1-cm² CuInSe₂/CdS device is already in the range of the better thin-film solar cell values.

*Work supported by the National Science Foundation (RANN).

[†]NSF Undergraduate Research Participant.

¹P. Yu, Y. S. Park, S. P. Faile, and J. E. Ehret, Appl. Phys. Lett. **26**, 717 (1975).

²S. M. Meese, J. C. Manthuruthil, and D. R. Locker, Bull. Am. Phys. Soc. **20**, 696 (1975).

³S. Wagner, J. L. Shay, P. Migliorato, and H. M. Kasper, Appl. Phys. Lett. **25**, 434 (1974).

⁴J. L. Shay, S. Wagner, K. Bachmann, E. Buehler, and H. M. Kasper, Proc. 11th IEEE Photovoltaics Spec. Conf. Phoenix, pp. 503–507, 1975 (unpublished).

⁵B. Tell, J. L. Shay, and H. M. Kasper, J. Appl. Phys. **43**, 2469 (1972).

⁶L. L. Kazmerski, M. S. Ayyagari, G. A. Sanborn, and F. R.

White, J. Vac. Sci. Technol. **13**, 139 (1976).

⁷See, for example, J. J. Loferski, J. Appl. Phys. **27**, 777 (1956).

⁸Unpublished at this time. For a description of an analogous system, see L. L. Kazmerski, M. S. Ayyagari, and G. A. Sanborn, J. Appl. Phys. **46**, 4865 (1975).

⁹See, for example, Paul Rappaport, Proc. Int. Workshop on Cadmium Sulfide Solar Cells and Other Abrupt Heterojunctions, Univ. of Delaware (AER75-15858), pp. 3–8, 1975 (unpublished).

¹⁰C. T. Sah, R. N. Noyce, and W. Shockley, Proc. IRE **45**, 1228 (1957).

¹¹C. T. Sah, IEEE Trans. Electron. Devices, ED-9, 94 (1962).

Bulk-hardened Sm-Co-Cu-Fe 2:17 magnets

A. Menth and H. Nagel

Brown Boveri Research Centre, CH-5401 Baden, Switzerland
(Received 26 April 1976; in final form 4 June 1976)

$\text{Sm}(\text{Co}_{0.87}\text{Cu}_{0.13})_z$ alloys were prepared with $7.2 \leq z < 8$. Homogenization heat treatment yielded single-phase 2:17 material for $z > 7.2$. For $z = 7.8$ some of the Co was substituted by Fe. Homogenized alloys remained single phase for up to 15% Co substituted. Remanence values B_R up to 12.1 kG were reached. Coercive fields H_C of 4 kOe were achieved by means of a low-temperature heat treatment. The magnetization process implies that pinning of the Bloch walls is responsible for the coercivity mechanism.

PACS numbers: 85.70.Nk, 75.60.Hn, 81.30.Cy

The hard magnetic potential of bulk and sintered RE (Co, Cu, Fe)_z alloys (RE = Ce, Sm, or Sm-Ce) with $5 \leq z \leq 7.2$ has been studied extensively in two different ranges: (a) the 1:5-type alloy with $5 \leq z \leq 5.6$,^{1–3} and (b) the two-phase mixture of 1:5- and 2:17-type alloys with $6 \leq z \leq 7.2$.^{4–9} Experimental and theoretical considerations^{9,10} have demonstrated that in these two-phase materials both the 1:5-type matrix and the primary 2:17-type phase exhibit a coercive field. These materials are precipitation hardened and rely on the pinning mechanisms of Bloch walls.^{11–13} The present paper reports the successful preparation of single-phase 2:17-type bulk samples with remanence values B_R above 11 kG, coercive fields H_C of 4 kOe, and rectangular demagnetization curves. Low-temperature heat treatment yields a well-defined maximum in the coercive field as a function of temperature.

The samples investigated were prepared in 120-g batches from 99.9% pure samarium, 99.999% pure copper, and 99.9% pure Co and Fe. Melting was done in boron nitride crucibles with i.f. heating under a protective atmosphere of argon. A cooling rate of about 50°C/min during the solidification of the melt yielded a coarse-grained material with an average grain size of about 2 mm. To homogenize the samples they were heat treated for several days in evacuated Ta-lined quartz tubes at temperatures of about 1200°C. The sealed samples were cooled from these temperatures by quenching in water. Annealing experiments below this temperature took place in Ta tubes in argon atmosphere. The compositions of the samples were checked by wet

chemical analyses of the loss by evaporation of samarium during the melting and annealing process.

Standard metallographic methods indicated single-phase 2:17 materials for $z = 7.5$ or 7.8 and with only

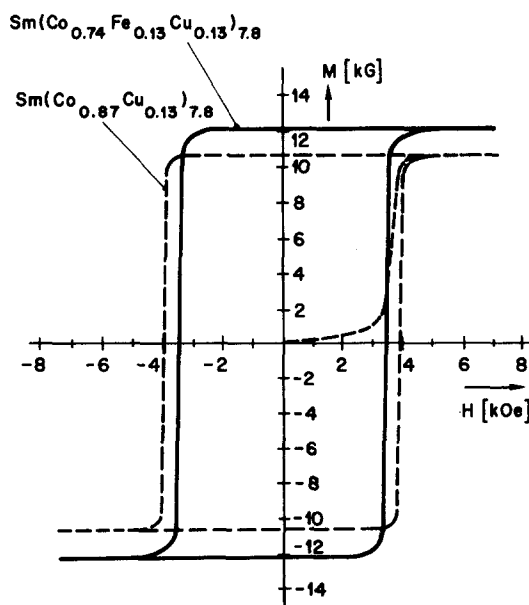


FIG. 1. Hysteresis loops of heat-treated single crystals of composition $\text{Sm}(\text{Co}_{0.87}\text{Fe}_{0.13}\text{Cu}_{0.13})_{7.8}$ and $\text{Sm}(\text{Co}_{0.74}\text{Fe}_{0.13}\text{Cu}_{0.13})_{7.8}$. Also shown is the "virgin" magnetization curve of the thermally demagnetized former sample.